Renewable Energy 93 (2016) 469 - 482

Effects of urban compactness on solar energy potential

Nahid Mohajeri[1*], Govinda Upadhyay[1], Agust Gudmundsson[2], Dan Assouline[1], Jérôme Kämpf, Jean-Louis Scartezzini[1]

[1*]Solar Energy and Building Physics Laboratory (LESO-PB), Ecole Polytechnique Fédérale de Lausanne (EPFL), 1015 Lausanne, Switzerland, e-mail: nahid.mohajeri@epfl.ch

[1]Solar Energy and Building Physics Laboratory (LESO-PB), Ecole Polytechnique Fédérale de Lausanne (EPFL), 1015 Lausanne, Switzerland.

[2]Department of Earth Sciences, Queen's Building, Royal Holloway University of London, Egham TW 20 0EX, UK.

Abstract

Compactness is a major urban form parameter that affects the accessibility of solar energy in the built environment. Here we explore the relation between various compactness indicators and solar potential in the 16 neighbourhoods (11,418 buildings) constituting the city of Geneva (Switzerland). The solar potential is assessed for building integrated photovoltaics (BiPV), solar thermal collectors (STC), and direct gain passive solar systems. The hourly solar irradiation on each of the building surfaces over one year period is calculated using CitySim simulations, while taking the effects of irradiation threshold for roof and facades into account. With increasing compactness, the annual solar irradiation decreases from 816 to 591 $kWhm^{-2}$. When passing from dispersed to compact neighbourhoods, the BiPV potential (given as percentage of total area) for facades decreases from 20% to 3%, the STC potential from 85% to 49%, and the passive solar heating potential from 21% to 4%, whereas for roofs the BiPV potential decreases from 94% to 79% and the STC potential from 100% to 95%. The solar potential for roofs, therefore, is much less affected than that for facades by the compactness. The results should be of great help for urban-form energy optimisation and building retrofitting interventions.

Keywords: urban density, renewable energy, entropy, sustainability, photovoltaics, solar thermal collectors

1. Introduction

Urban areas have expanded enormously in the past decades and are likely to do so in the coming decades. In many countries, they offer great opportunities for on-site energy production and use, thereby minimising the loss or transformation through energy transmission. Solar energy is one of the renewable energy resources with the greatest potential and could be the world's largest source of electricity by 2050 [1]. The rapid increase in the use of solar energy in recent years is highlighting its great development potential at present, and even more so as a future energy source [1, 2]. According to the International Energy Agency roadmap 2014, solar photovoltaics and solar thermal energy could contribute to 27% of the global electricity production by 2050 [1], if the expected technological progress and required policy actions will occur. In addition to its being renewable and a carbon-dioxide (CO_2) neutral energy system [3], solar energy has one very obvious benefit, namely that the location of the energy source is commonly the same as the location of the energy use. This applies in particular to solar energy in urban areas, where building envelopes, walls and roofs, are used to capture and transform the solar irradiation into heat and /or thermal energy or electricity.

Quantifying the global solar irradiation reaching building envelopes and assessing their potential for active (photovoltaic electricity production and solar thermal for space/water heating) and passive solar heating have received much attention in the past decade [4, 5, 6, 7]. Active solar systems use mechanical and electrical devices to convert solar radiation to heat and electric power. Passive solar systems, by contrast, uses building design (e.g. thermal mass) to capture the sun's heat and to reduce the energy use for space heating and, possibly, for cooling. In particular, there have been several studies on the effects of urban form on the solar energy potential [4, 8, 9, 10, 11, 12] on scales varying from building and neighbourhood to urban and regional scale [5, 13, 14, 15] using simulation and statistical methods [7, 12]. While these studies have made significant progress in the topics they address, they primarily explore the effects of urban form on solar potential using generic models of urban layouts [10]. Some studies focus on solar potential only in residential buildings [11, 16] using a limited number of buildings, while others investigate the effects of urban form on solar potential for new buildings in their early-design phase [11, 17]. Also, several methods have been used to improve the design of new urban settlements by optimising size and shape of buildings for the utilisation of solar irradiation [18, 19].

Urban compactness is one of the most commonly used urban form indicators. The effects of urban compactness on solar potential have, however, rarely been studied in a comprehensive way for the real built environment. Although compactness is used in many studies and assessed in many ways [11, 12, 20], we still have little information as to how compactness of existing neighbourhoods limits the solar potential of their buildings. In addition, we do not know the most efficient technology for harnessing the solar energy potential for roofs and facades in compact urban areas.

Here we address the effects of urban compactness on solar potential as regards various solar-energy technologies. Our results provide a framework that should be of great help in the decision-making process for assessing and integrating solar potential in dense built environment. The focus is on estimating active and passive solar gains associated with building roofs and facades using CitySim for hourly solar irradiation simulation. Sixteen neighbourhoods in the city of Geneva are used as a case study to evaluate the effects of compactness indicators on the solar potential. A sensitivity analysis is also performed to illustrate the effects of different annual solar irradiation thresholds on the energy potentials of facades and roofs. The results provide guidelines for urban-form optimisation in relation to retrofitting interventions on building envelopes and solar-energy applications in dense urban areas.

2. Data and methods

While the methods introduced and elaborated in this paper are completely general and applicable to other urban areas, all the data used and analysed are from the city of Geneva in Switzerland (Fig. 1). Geneva is located at 46°12' North, 6°09' East, at the south-western end of Lake Geneva, where the lake flows

back into the Rhône River. It is surrounded by two mountain chains, the Alps and the Jura. The average altitude of Geneva above sea level is 374 m. The city, with a population of about 195 thousand in 2013 (www.bfs.admin.ch), is the second largest in Switzerland and the largest one in the French speaking part of the country. The city is composed of 16 neighbourhoods or zones with a total of 11,418 buildings (Fig. 1). The total area of the city is about 16 km^2 with a population density of 12,000 per km^2. About 92% of the total land in the city is used for built up area, out of this about 50% are buildings.

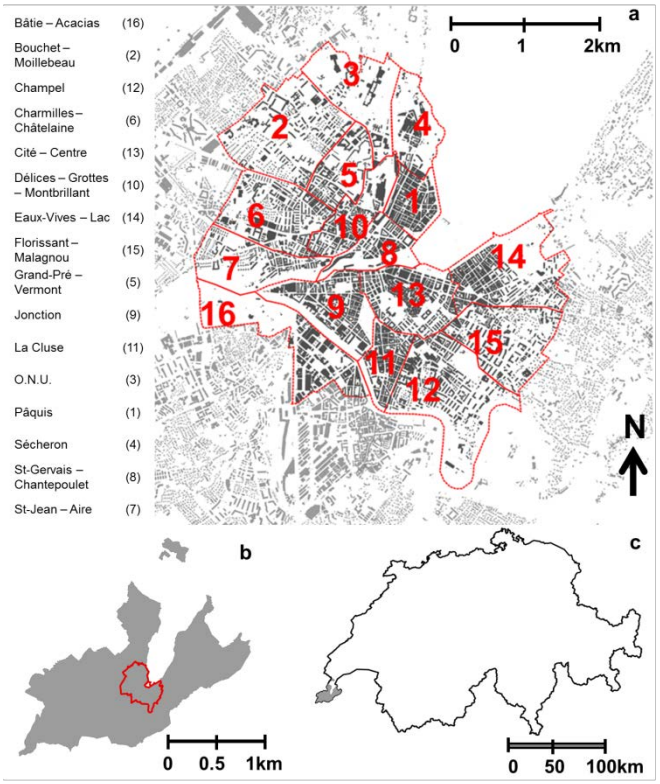

Figure 1. (a) Building map of the city of Geneva, composed of 16 neighbourhoods, each one marked by broken red line. (b) The location of Geneva city (shown by red, solid and closed curve) in the canton of Geneva. (c) The location of canton of Geneva in Switzerland.

2.1. Compactness indicators

Several compactness indicators are used to assess the availability of the solar potential in the 16 neighbourhoods. These indicators are (Fig. 2): (a) volume-area ratio, (b) site coverage [5, 6, 9, 10, 11, 12, 16, 17], (c) plot ratio [5, 6, 9, 10, 11, 12, 16, 17], (d) building density [15], (e) population density [15], and (f) nearest-neighbour ratio [12]. The indicators are shown schematically in Fig. (2), and explained as follows: (a) Volume-area ratio is the total building volume in a neighbourhood divided by total area of a neighbourhood. (b) Site coverage is the total built area in a neighbourhood divided by total area of a neighbourhood. (c) Plot ratio is the total floor area in a neighbourhood divided by total area of a neighbourhood. (d) Building density is the total number of buildings in a neighbourhood divided by total area of a neighbourhood. (e) Population density is the total number of people living in a neighbourhood divided by total area of a neighbourhood. (f) Nearest-neighbour ratio is the average distance between buildings from centroids normalised by the total area of a neighbourhood. If the ratio is less than 1, the building configuration indicates clustering; if the ratio is greater than 1, the configuration is more uniformly distributed.

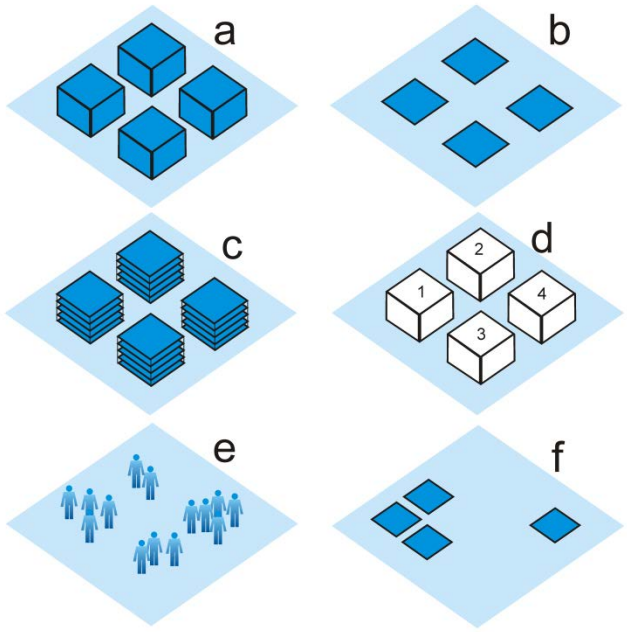

Figure 2. Schematic presentation of how different indicators of urban compactness are calculated. (a) Volume-area ratio, (b) Site coverage, (c) Plot ratio, and (d) Building density, (e) Population density, (f) Nearest-neighbour ratio.

While all indicators are a measure of the degree of compactness, they show different aspects of urban configuration and are thus complementary. For example, (a) volume- area ratio (Fig. 2a), which is the ratio of total building volume in a site to the total site area, shows building heights and is a 3D

representation of compactness. It is a vertical distribution of built forms. (b) Site coverage is the proportion of a site that is covered by building footprints. This is a 2D representation (Fig. 2b) of urban compactness or a horizontal distribution of built forms. More specifically, the higher the site coverage the lower open space available on the site. (c) Plot ratio captures the total gross floor areas per unit area of the site. It is regarded as a standard indicator for the regulation of land-use zoning and development control. It is critical ratio for evaluating building solar facades. (d) Population density (the number of people per unit of area) and (e) building density (number of building per unit of area) indicate the distribution of people or buildings in the entire area. (f) Nearest-neighbour ratio is an indication of horizontal distribution of buildings but it is different from site coverage. If the ratio is less than 1, the buildings are clustered; if the ratio is greater than 1, the buildings are more uniformly distributed.

The compactness indicators or measures show large variations in intensity or values throughout the city, that is, between the 16 neighbourhoods (Fig. 3). Yet, most of the indicators vary in harmony within the city. For example, the volume-area ratio, site coverage, plot ratio, and building density all have their highest values in neighbourhoods or zones number 1 and 11, and to a lesser degree in zone 13 (Fig. 3). By contrast, zones 3 and 16, and to a lesser degree 4 and 7, have all very low indicators. The population density (Fig. 3e) shows also similar, yet somewhat different, variation. The highest values are for neighbourhoods 11 and 1, with 10 and 6 somewhat lower, although still high. The lowest population densities are, as for the other indicators, in neighbourhoods 3 and 16, but also in 9 and 13. The nearest neighbour ratio varies from 0.6 to 1.10. The highest values are for neighbourhoods 1 and 11, followed by 6, 13, 10, in that order, indicating a uniform spatial distribution of buildings. As indicated above, ratios below 1 indicate clustering of building to a certain degree.

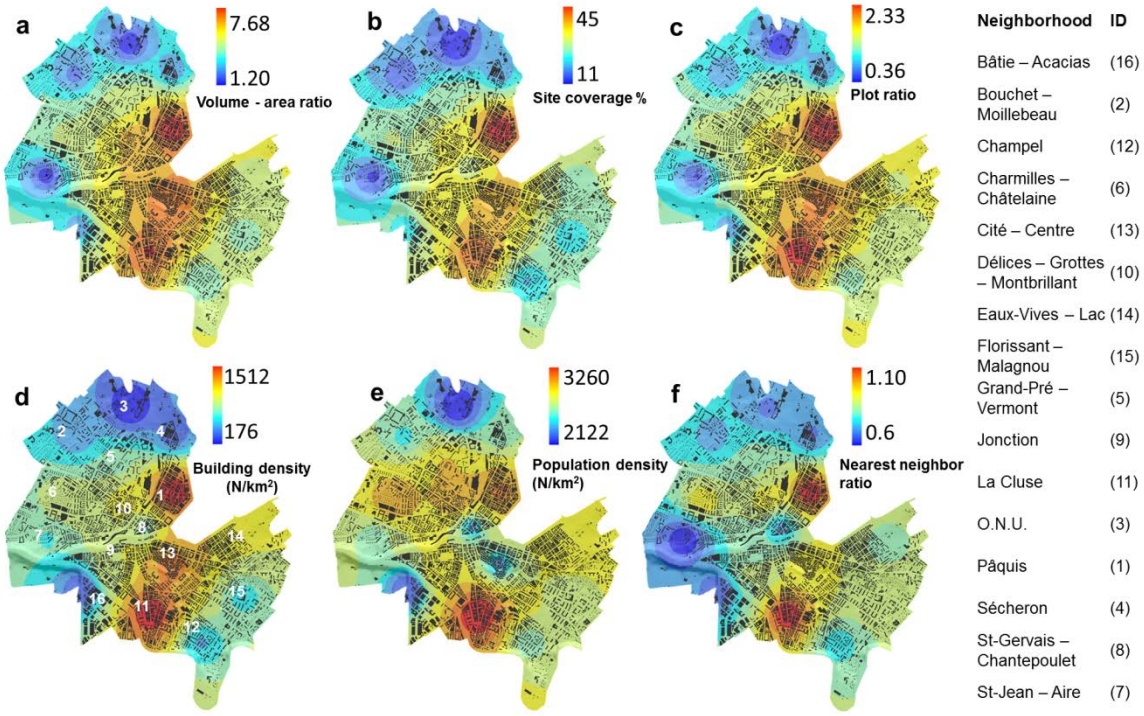

Figure 3. Variation of urban compactness indicators between different neighbourhoods (name and associated number for each neighbourhood are given) in the city of Geneva. (a) Volume –area ratio; (b) Site coverage in percentage; (c) Plot ratio; (d) Building density; (e) Population density; (f) Nearest neighbour ratio.

We propose another urban compactness indicator, that is, entropy. Entropy, denoted by S, is a fundamental concept in statistical physics (and classical thermodynamics), and information theory [21, 22, 23, 24, 25]. In statistical physics and information theory, entropy has a probability basis and can thus be used for analysing the probability distributions of building sizes, including area, perimeter, volume, and height [26, 27]. The following expression, referred to as Gibbs – Shannon entropy equation (the difference between the expressions of Gibbs and Shannon relates to the units of the constant *k*), gives the entropy for a general probability distribution as:

$$S = -k\sum_{i=1}^{t} p_i \ln p_i \qquad (1)$$

where t is the number of classes or bins with nonzero probabilities of certain building size, and p_i is the probability of building size belonging to the i-th bin. The minus sign for k is justified by the fact that a probability must be between 0 and 1, and the natural logarithm of numbers between 0 and 1 is negative. Thus, a minus sign for k ensures a positive value for the entropy. When calculating the entropy using Eq. (1), only the bins with at least one measured building size are included, that is, only those bins where the probability of finding a size is greater than zero. We also have that:

$$\sum_{i=1}^{t} p_i = 1 \qquad (2)$$

Equation (2) means that the sum of the probabilities of all the bins equals one. Equation (1) can be interpreted in terms of dispersal or its reciprocal, compactness.

2.2. Solar irradiation modelling

For data management we use PostgreSQL, a complete and open-source database management systems (DBMS), which offers a wide range of conventional SQL functionalities for data handling together with PostGIS extensions for geometrical objects handling. A PostgreSQL database was initially developed for the city of Neuchâtel [28] and modified for the city of Geneva [29] so as to provide input for the CitySim simulations of the hourly solar irradiation for the 11,418 buildings. The PostgreSQL database consists of various tables, each containing essential information about the objects (e.g. building footprints, wall types, materials) so as to create an input file for the simulation. A program in JAVA programming language, called CDL (CitySim Database Linker), was written to retrieve data stored in the database and to create the input XML file for CitySim. The program makes use of the building footprints together with their average height to reproduce a three-dimensional shape for the buildings, distinguishing roofs and facades. Urban objects such as roads and trees were not modelled in order to keep a reasonable amount of surfaces in the scene and also to reduce simulation time. For hourly solar irradiation simulation (8760 hour in a typical year), sixteen XML files were made for the 16 neighbourhoods, each retrieving information of several hundred buildings (Table 1). Figure 4 shows the CitySim simulation results for the annual solar irradiation for the 16 neighbourhoods of the city of Geneva. The solar irradiation ($kWhm^{-2}$) in CitySim is estimated hourly for all the building roofs and facades for a typical year.

The annual solar irradiation ($kWhm^{-2}$) for each neighbourhood is calculated based on the hourly average solar energy (kWh) of all the building surfaces in that particular neighbourhood over the cumulative surface area of the buildings (Fig. 4). In both SUNtool, which is CitySim's predecessor [30, 31], and in CitySim itself [32] the simplified radiosity algorithm was used to calculate the incoming shortwave irradiation on building surfaces including the inter-reflections with scene surfaces. The weather data for one year period used in this simulation was obtained from Meteonorm (www.meteonorm.com). Weather data consists of hourly values of air temperature, wind speed and direction, humidity, precipitation, diffuse horizontal irradiance, and beam normal irradiance. The solar irradiation model in CitySim solves for beam, diffuse and reflected irradiance using complex modelling techniques based on Perez all-weather model [33] and simplified radiosity algorithm [30] for inter-reflections. It is worth noting that this radiation model has been validated by inter-model comparison with RADIANCE [30].

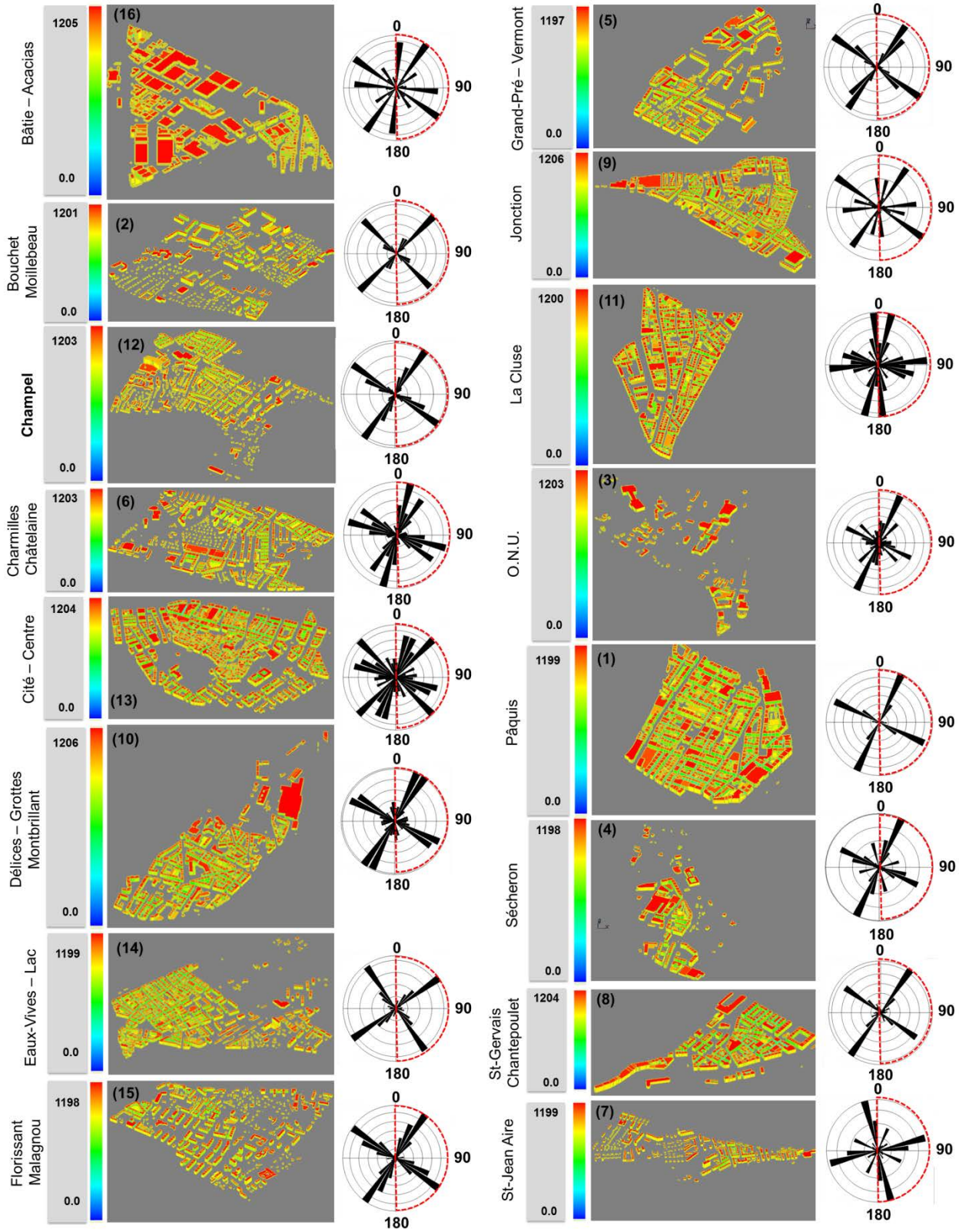

Figure 4. Annual solar irradiation, kWhm^{-2} (the colour bars shows the minimum and maximum values) estimated using CitySim and facade orientations for 16 neighbourhoods in the city of Geneva

2.3. Building orientation

The orientation of a building partly determines the intensity of the incoming solar irradiation [5, 11]. We measured the orientation of all buildings in the 16 zones in the city of Geneva (Fig. 4). The building data is from Swisstopo (www.swisstopo.admin.ch) and we use ArcGIS 10.2 to calculate the azimuth angles of the building sides (www.esri.com) as well as the side lengths by segmentation of building polygon into polyline. The azimuths for each side of the building were calculated in ArcGIS and the program GEOrient (www.holcombecoughlinoliver.com) is used for analysing and visualising the results. Rose diagrams can be constructed using either normalised (weighted) or non-normalised (unweighted) data. The orientations of the sides of buildings are non-normalised when all sides count equally in the rose diagrams but normalised when more weight is given to the long sides, which are then considered as composed of many short parts. Here we use normalised orientations so that the side lengths are taken into account (Fig. 4).

3. Results and discussion

The main results as regards the global horizontal irradiation on the building envelope (roofs and facades) as well as active and passive solar systems to convert solar irradiation to heat or electric power on roofs and facades for 16 neighbourhoods in the whole city of Geneva are presented and discussed. The results have general implications for the dense built environment in other urban areas, especially those with climatic conditions similar to Geneva.

3.1. Annual solar irradiation of neighbourhoods and urban compactness

We compared the six indicators, namely site coverage, volume-area ratio, plot ratio, building density, population density, and nearest neighbour ratio with the annual solar irradiation received by the 16 neighbourhoods in Geneva. We use least-square regression models to seek the relations between the irradiation, on one hand, and the compactness metrics, on the other hand, using the coefficient of determination (R^2) as a measure of how well the irradiation can be explained in terms of the indicators (Fig. 5; Table 1). The significance of the relations is discussed in relation with p-values. The p-value is a percentage that indicates the probability that the coefficients *a* and *b* in the regression equation $y = a + bx$ are not obtained by chance. For example, if $p < 0.05$ then there is less than 5% chance that the observed linear relationship emerged randomly.

The results (Fig. 5, Table 1) show strong negative linear correlations between site coverage, volume area ratio and plot ratio, on one hand, and the annual solar irradiation ($kWhm^{-2}$), on the other.

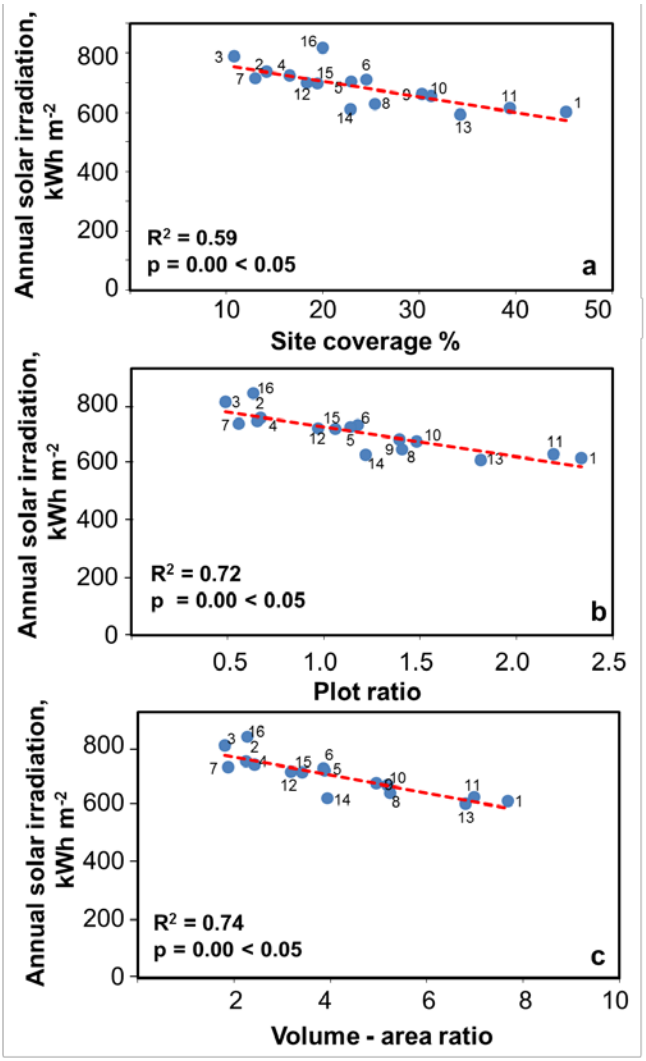

Figure 5. Annual solar irradiation ($kWhm^{-2}$) versus (a) site coverage, (b) plot ratio, (c) volume-area ratio for the 16 neighbourhoods. The coefficient of determination (R^2) and the associated significance (p-value) at 5% are given for each linear correlation.

All these indicators are a measure of compactness; that is, the higher the indicator, the more compact is the neighbourhood. However, each

compactness indicator applies to different aspects of the built form configurations [34, 35]. For example, the site coverage is a percentage of land area covered by the buildings, whereas the plot ratio is a measure of intensity of the use of built area. The volume - area ratio is also a measure of intensity and has a unit of length, indicating the building height. The coefficient of determination between the indicators and the solar irradiation varies from 0.59 (site coverage) to 0.74 (volume-area ratio). Thus, 59-74% of the variation in the solar irradiation received by the urban areas of Geneva can be correlated with (or predicted based on) variation in these indicators. Generally, the neighbourhoods with a compact block configuration (e.g. number 1, 8, 9, 10, 11, 13 in Figs. 4 and 5) receive less solar energy than neighbourhood with detached and terraced configuration (number 2, 6, 7, 12, 15) due to the effects of shading from neighbouring buildings. Of the three indicators, the volume – area ratio shows the best correlation with the annual solar irradiation.

To test further the effects of urban compactness on the potential of solar energy, we compared the average building density with the annual solar irradiation in Geneva (Fig. 6). Measurement of building density with respect to number of buildings per unit land area is an important indicator, particularly for the policy making in infrastructure planning.

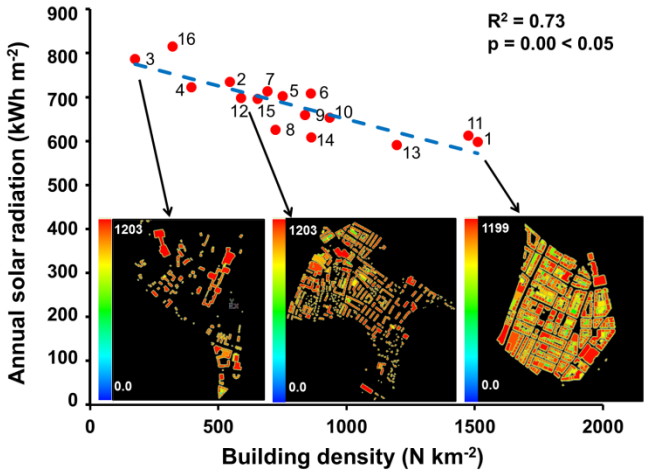

Figure 6. Annual solar irradiation (kWhm^{-2}) versus building density (number, N, per square kilometre) for the 16 neighbourhoods. Three neighbourhoods have shown as an example. The coefficient of determination (R^2) and the associated significance (p-value) at 5% are given for the linear correlation.

The results show that as the building density increases, the solar irradiation decreases. This means that the more compact neighbourhoods receive proportionally less solar irradiation. The mutual shading of buildings in the compact urban blocks (e.g., in neighbourhoods number 1, 11, 13) with high building density limit the accessibility of building surfaces, particularly the facades, from receiving much solar radiation. The effects of mutual shading, however, in the neighbourhoods with detached and terraced configuration, and thus having low building density, is much less. The coefficient of determination (R^2) is 0.73, so that 73% of the variation in solar irradiation can here be related to variation in the building density.

Population density and nearest neighbour ratio (Fig. 2) are also indicators of compactness. As these indicators increase the annual solar irradiation decreases. The coefficients of determination (R^2) for population density and nearest neighbour ratio in relation to annual solar irradiation, however, are relatively low, 0.33 and 0.48, respectively. Thus, the population density may not be a reliable indicator for solar potential. Regarding the nearest neighbour ratio, the higher the indicator the more uniformly distributed the buildings are and the lower the solar potential. The reason is partly related to high site coverage and also high plot ratio. The buildings in neighbourhoods of 1, 11, 10, 13 are uniformly distributed, as indicated by the high nearest neighbour ratio, while having high site coverage and plot ratio – therefore less solar potential. However, there are some exceptions. Neighbourhood 6 (Table 5), with uniformly distributed buildings, has relatively high solar potential (nearest neighbourhood ratio is 1.01 and annual solar irradiation is 708 kWhm^{-2}). The reason is partly related to the moderate site coverage and plot ratio, which implies considerable spacing between buildings, that is, comparatively dispersed buildings and thus high solar potential.

The annual solar irradiation increases with distance from the old centre, the core of Geneva (Fig. 7). The coefficient of determination (R^2) is 0.61 (at 0.05 significance level), suggesting that the annual solar irradiation increase as we move away from the old core to the suburb of the city. The results also imply that spread or dispersed (less compact) neighbourhoods, mostly located in the suburbs, receive more solar energy. The six

indicators of urban compactness for Geneva, discussed above, all indicate that increasing compactness decreases the solar energy potential. However, they measure different aspects of the urban configuration and are thus complementary.

Out of 6 indicators 4 have clear effects on annual solar irradiation (Figs. 5 and 6). Although these indicators are among the most common measures of urban compactness, we introduce another, and very flexible, indicator, namely urban entropy.

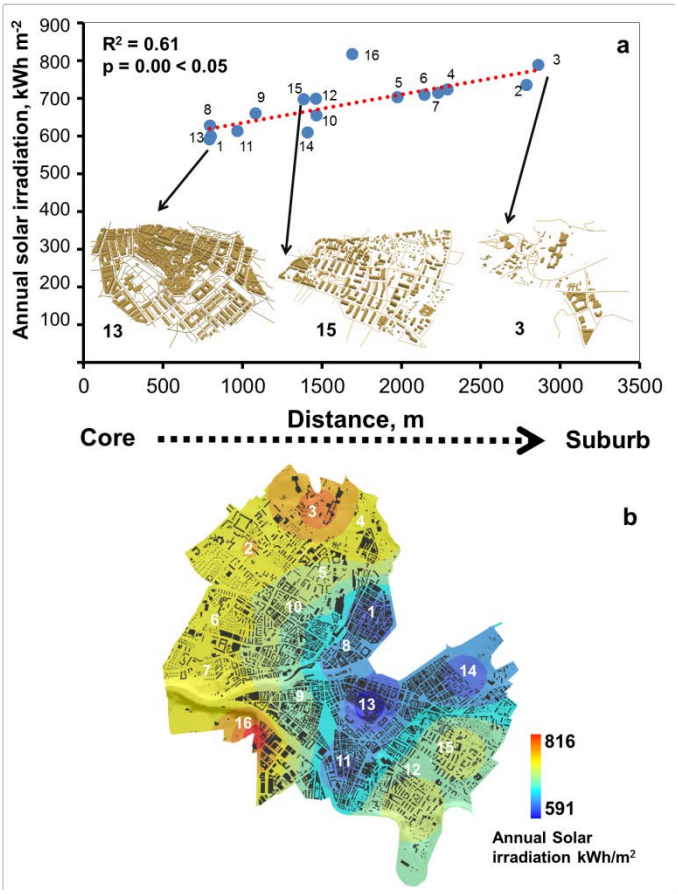

Figure 7. (a) Variation in annual solar irradiation for the 16 neighbourhoods with distance from the centre of the city of Geneva. The coefficient of determination (R^2=0.61) and the associated significance (p-value) at 5% are given for linear correlation. (b) Distribution of annual solar irradiation (kWhm^{-2}) within the 16 neighbourhoods in Geneva.

3.2 Solar potential and urban entropy

As indicated above, entropy is a quantitative measure of size distributions of various indicators (e.g. areas, perimeter, height, and volumes) of the buildings. More specifically, entropy, as used in statistical physics and information theory, is a measure of dispersal or spreading, that is, of the shape of the associated probability distribution. In the present context, entropy is a measure of the dispersal or spreading of the probability distributions of the various building geometry.

The entropies of all the probability distributions associated with the building geometries in Geneva, that is, for the building area, perimeter, volume, and height are given in Table 2. Building area, perimeter, and volume all follow heavy-tail size distributions [26].

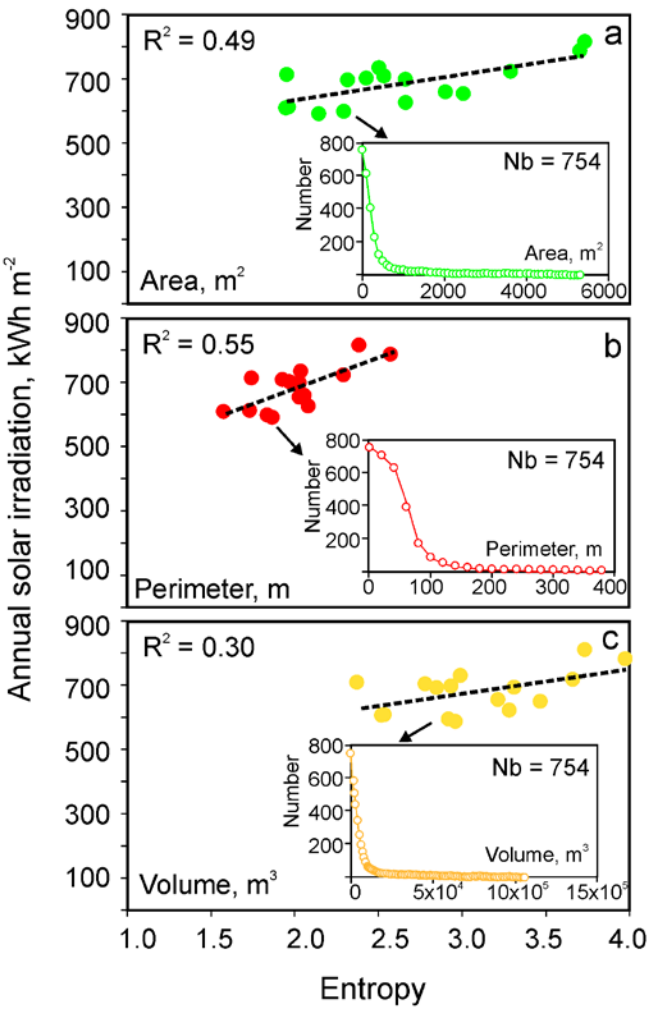

Figure 8. Annual solar irradiation as a function of entropy. Annual solar irradiation increases as the entropies of area, perimeter, and volume increase. The insets show heavy-tail distributions of building area, building perimeter, and volume in one neighbourhood, with a total of 754 buildings, as an example.

By contrast, the height of buildings in Geneva has a bimodal size distribution. The average values of all these four parameters (area, perimeter, volume, and

height) in the 16 neighbourhoods of Geneva show linear correlations with entropy; that is, the greater the average area, perimeter, volume and height of buildings in a given neighbourhood, the greater is the entropy (Table 3) [26].

Here the entropy is calculated for the building size distributions (area, perimeter, and volume), as indicated by Eq. (1). The results (Fig. 8) show that the greater the entropy of the building size in each of the 16 neighbourhoods, the greater the dispersal, and the greater is the annual solar irradiation received by the buildings in that neighbourhood. Insets in Fig. 8 (one neighbourhood as an example) show the building area, perimeter, and volume follow heavy-tail size distribution. However, the building heights follow a bimodal distribution (Fig. 9; Table 2). While there is no clear relation between entropy of building heights and annual solar irradiation, the average of building heights in each neighbourhood has a strong negative relation with the annual solar irradiation (R^2 = 0.64). The greater the average height, the lower the solar potential, particularly in neighbourhoods with high site coverage where the solar access on façade is limited (Fig. 9).

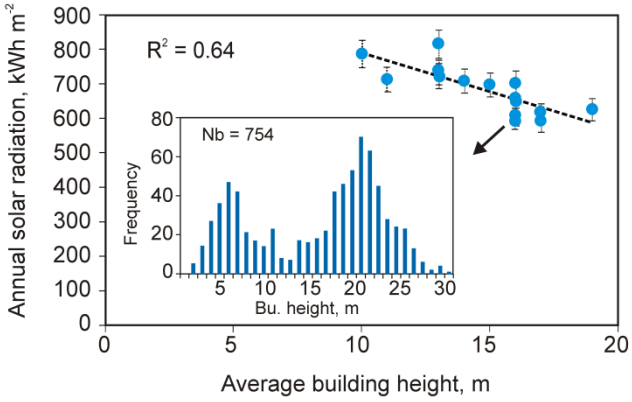

Figure 9. The negative relation between annual solar irradiation (kWhm^{-2}) and average building heights. The inset shows a bimodal distribution of building heights in one neighbourhood, with a total of 754 buildings, as an example.

The greatest average height of buildings occurs in the most compact neighbourhoods. We have already shown that increasing compactness decreases the solar irradiation so that increasing average height is also correlated with low solar energy potential, as indeed Fig. 9 shows. In addition, entropy calculations for building heights show a very limited range, from 2.92 to 3.30, indicating that little variation in building heights between neighbourhoods.

The more peaked the probability distribution of building orientation (Fig. 10; neighbourhood 1), the lower is the entropy. By contrast, the more dispersed or uniformly distributed the building orientations, the higher is the entropy. Although the results show that there is no clear relation between entropy of building orientation and annual solar irradiation (Fig. 10; Table 2), the impact of building orientation on solar energy depends on compactness. For example, distribution of building orientation and associated entropies in the two neighbourhoods 1 (S = 2.97) and 13 (S = 3.46) vary considerably, whereas both neighbourhoods have similar annual solar irradiation, namely, 598 and 591 kWhm^{-2} respectively. The similarity in irradiation, despite variation in orientation entropy, is due to the high compactness of these neighbourhoods as defined by plot ratio, site coverage and volume-area ratio.

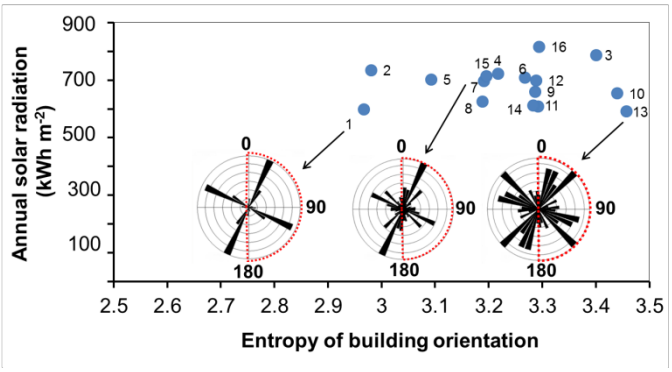

Figure 10. The relation between annual solar irradiation (kWhm^{-2}) and entropy of building orientations. The rose diagrams of building orientations in three neighbourhoods are shown as examples.

3.3 Solar potential for different energy conversion methods

Here we discuss three main technologies for the energy conversion of solar irradiation in relation to their potential for Geneva. These are (1) building integrated photovoltaic systems (BiPV or just PV for short) and (2) solar thermal collectors (STC), both of which are active systems, and (3) direct gain passive solar systems.

The effectiveness of solar active and passive techniques were estimated separately for roofs and facades. A Python script was written to separate hourly solar irradiation values (8760 hours) for roofs and facades. We apply irradiation threshold values for solar PV (roof and facade), STC (roof and facade) and passive systems (facade) established by [4] and [36] for Switzerland. The threshold values area calculated based on the technical limitation as well as economic factors (Fig. 11).

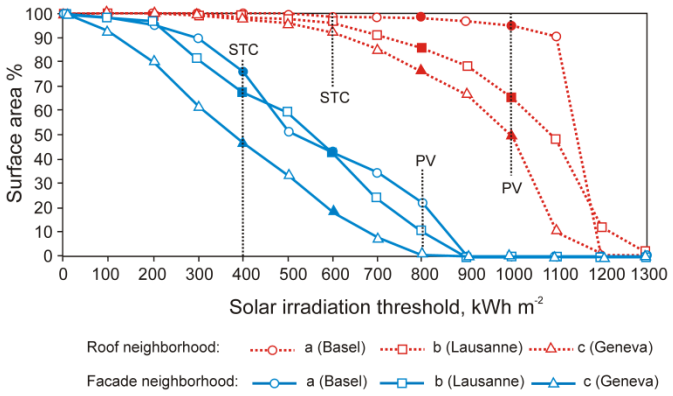

Figure 11. Usable surface area, in percentage of the total, as a function of active solar technology energy thresholds for three cities in Switzerland. The red broken lines indicate the solar irradiation threshold for roofs and the blue solid lines show the solar irradiation thresholds for facades. The vertical lines show threshold values for PV and STC on roof and facade (modified from Robinson et al., 2005).

These threshold values have been used in several studies [11, 16], but can easily be adapted according to technical innovation and economic progress of solar technologies in the future for different countries. A threshold value indicates the minimum amount of annual radiation required for active solar technologies and the minimum amount of winter radiation required for passive solar techniques to be economically viable at a particular location. The potential for the various technologies is calculated as the relative fraction (percentage) of the roofs and facades of the buildings that can be used for the particular solar energy conversion systems. The percentage is based on an hourly solar irradiation threshold PV value for roof of 1000 kWh m^{-2} and for façade of 800 kWh m^{-2}. Similarly, the threshold STC value for roof is 600 $kWhm^{-2}$ and for façade 400 $kWhm^{-2}$. Passive solar potential for space heating is calculated based on winter season considering the threshold value of 187 $kWhm^{-2}$ (Fig. 11; Tables 3 and 4).

Using heating season degree-days (*DD*) for the city of Geneva (3151 *DD*), the threshold value for passive solar (or thermal) heating (PSH) can be determined as follows:

$$PSH = 0.024 \times DD \times \frac{U}{g\eta} \quad (3)$$

where U is glazing thermal transmittance ($Wm^{-2}K^{-1}$), g is solar heat-gain coefficient of windows, and η is solar gain utilisation coefficient. The result for passive solar (or thermal) heating, *PSH*, is given in $kWhm^{-2}$. For a typical double glazing window and Switzerland climate conditions, U is equal to 1.3, g is equal to 0.75, and η is equal to 0.7 (Robinson et al., 2005), which are the values used here.

3.3.1 Active and passive solar accessibility in relation to plot ratio and building orientation

We classified the 16 neighbourhoods by increasing plot ratio and entropy of building orientation along the x-axis (Fig. 12). The y-axis shows the percentage of BiPV and STC yields as well as the passive solar potential that are above the thresholds, for each neighbourhood. For all the solar energy technologies, accessibility for roof and facades generally increase as the plot ratio decrease. Although the passive solar potential and BiPV facade are very similar and low, the potential for STC facade is relatively high. In addition, the potential for both roof integrated PV and roof integrated STC systems is very high (Fig. 12a; Table 3). More specifically, the PV potential for roof increases from about 79% to 94% with decreasing plot ratio. Similarly, the STC potential increases from 95% to about 100% for the roof areas. The potential for the STC systems on roofs and facades is considerably higher, however, than that for the PV systems. For the facades, the STC system potential ranges from about 49% to about 85%, but is overall much lower than that for the roofs. The general trend for STC potential is increasing with decreasing the plot ratio, but there are some fluctuations. The PV potential for facade shows some fluctuations with decreasing the plot

ratio, but generally ranges from 3% to 20%. Similarly, the passive solar heating potential for the façade ranges from 4% to 21%, so very similar to the PV potential for the façade.

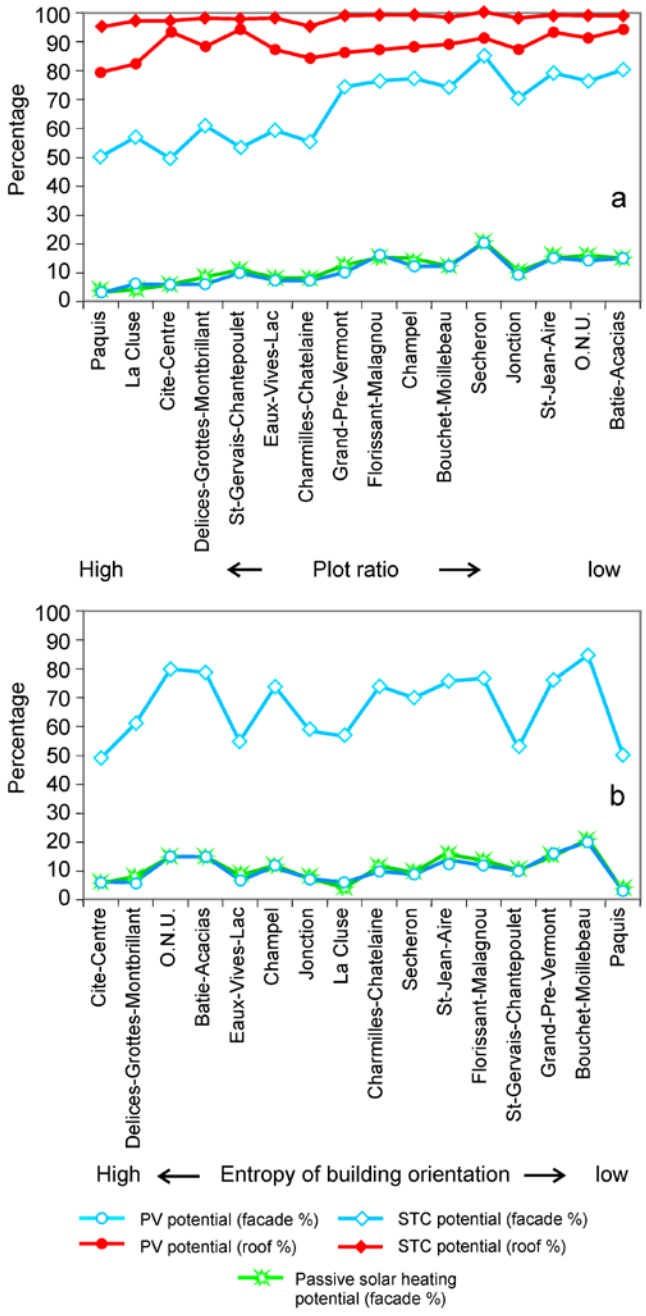

Figure 12. Comparison of relative fraction of building facade and roof areas appropriate for a given solar technology (PV, STC, passive) in the 16 neighbourhood of the city of Geneva. The neighbourhoods are ranked based on (a) plot ratio and (b) entropy of building orientation.

The dispersion in building orientations, as explained before, are quantified using the entropy indicator. There is no obvious trend for the solar potential harvested by different technologies as the dispersal of building orientations decreases (Fig. 12b). However, a comparison of building orientations and plot ratio with the solar accessibility indicates that the density has a larger impact than the building orientation. The effect of shading in lowering the solar potential is generally strong. This is particularly so in dense or compact neighbourhoods - as measured by plot ratio - even for buildings with favourable orientation. For example, buildings in Paquis and Bouchet-Millebeau are favourably oriented and have also low entropy. In Paquis, the solar potential for both roof and facade is very low due to the high plot ratio and mutual shading effects, whereas Bouchet-Millebeau, with a medium plot ratio, has a relative high solar potential for roofs and facades (Figs. 4, 12). The effect of building orientation is also less in more dispersed neighbourhoods. In Cite-Centre and O.N.U. building orientations are dispersed and with high entropy. However, the solar potential in Cite-Centre, which has a high plot ratio, is much lower than in O.N.U., which has a low plot ratio. The results underline that density or compactness has much greater effects on solar potential than some other urban-form parameters such as orientation.

3.3.2 Active and passive solar accessibility in relation to urban compactness

We analysed further (Fig. 13, Table 3) the relation between several compactness indicators and solar potential for roofs and facades, for both passive and active technologies. It is clear that all the lowest percentages of solar potential for roofs and facades occur in the relatively compact neighbourhoods (Fig. 13). There are clear negative linear correlations between the indicators plot-ratio, volume-area ratio, site-coverage, and building density on one hand, and the percentage of roofs and facades available for BiPV, STC, as well as the direct gain passive solar systems, on the other hand (Fig. 13). The PV potential for facades is low in all neighbourhoods with high plot-ratio, volume-area ratio, site-coverage, and building density, considering the threshold value above 800 kWh m^{-2}. Among the compactness indicators, site coverage has the highest effect on facade PV potential.

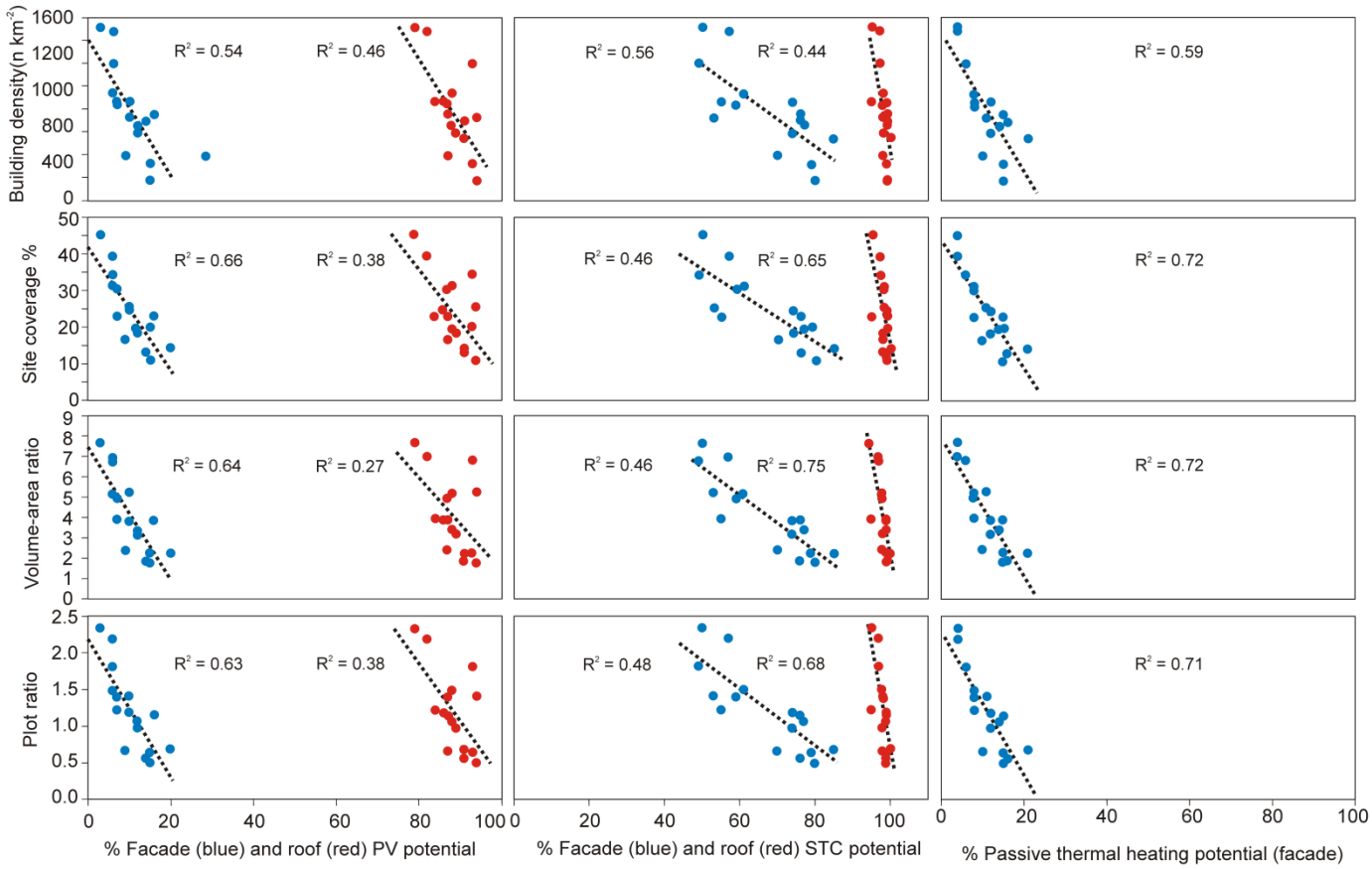

Figure 13. Relation between urban compactness indicators (site coverage, volume-area ratio, plot ratio, building density) and fraction of building facade and roof areas appropriate for a given solar technology (PV, STC, passive) in the 16 neighbourhoods of the city of Geneva. The coefficient of determination (R^2) are given for each linear correlation (significance level is at 5%).

The PV potential for facades decreases from 20% in low compact area to 3% in high site coverage area. Generally, the relations between the PV potential on the roof and various compactness indicators are not strong, indicating that the PV potential on roofs are not affected much by the compactness when the threshold value is above 1000 kWh m^{-2}. The PV potential on roofs, however, varies from 94% in dispersed areas to 79% in compact areas. The lowest coefficient of determination (R^2 = 0.27) is between volume-area ratio and roof PV potential.

The STC potential for facades is affected by the urban compactness, decreasing from 85% in dispersed neighbourhoods to 49% in compact neighbourhoods. The threshold value for STC façade potential is 400 kWhm^{-2}. There is a strong relation between STC facade potential and building density, as measured by number of building per unit area (R^2 = 0.56). Although, the STC for roofs are strongly related to the urban compactness, the range is very narrow or from 100% in dispersed areas to 95% in compact areas. For the threshold value used here, 600 kWh m^{-2}, there is a strong relation between STC roof potential and volume-area ratio (R^2 = 0.75). The passive solar potential for facade, using the threshold value of 187 kWh m^{-2}, has strong relation with all urban compactness indicators. The range, however, is narrow with the passive thermal potential decreasing from 21% in dispersed areas to 4% in compact areas.

3.4 Sensitivity analysis of solar potential

As indicated above, the threshold PV value for roofs is 1000 kWhm^{-2} and for facade 800 kWh m^{-2}, whereas that for STC for roofs is 600 kWhm^{-2} and for facade 400 kWhm^{-2}. Similarly, for passive solar heating the threshold value is 187 kWhm^{-2}. These threshold values, used in this study (Figs. 12 and 13), are partly based on technical limitations and economic considerations [4].

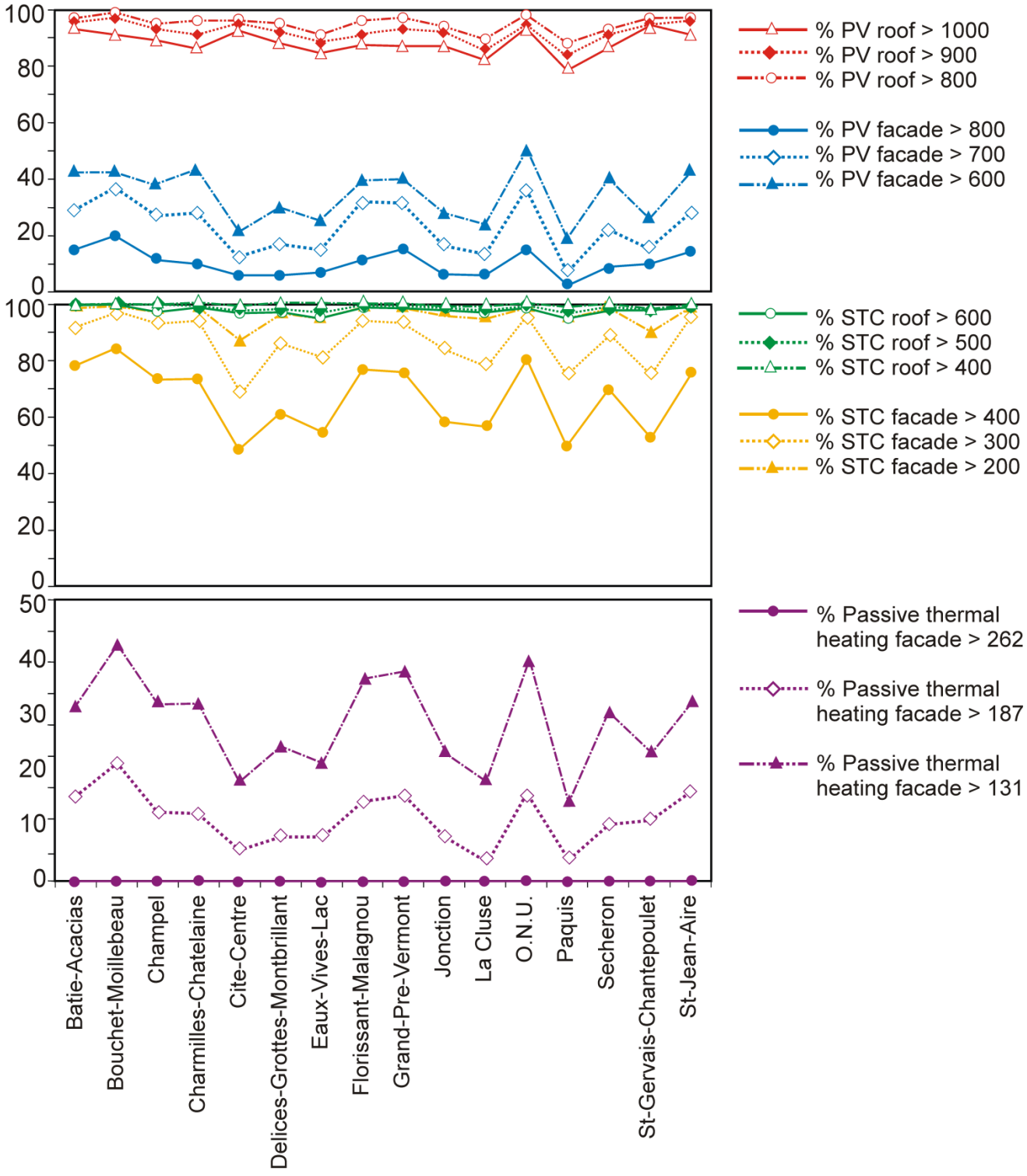

Figure 14. Sensitivity study of the threshold values of annual solar irradiation ($kWhm^{-2}$). The annual solar irradiation is calculated based on the threshold values in Table 4, so as to compute the potential for the corresponding solar techniques.

As the cost of solar technologies particularly PV solar modules reduced dramatically since 2004, a standard sensitivity analysis is proposed so that to test alternative thresholds suggested by [4, 36] (Fig. 11) for roof and facades of passive and active solar potentials (Fig. 14). The results for roof-integrated PV show that as the thresholds are lowered from 1000 kWh m^{-2} to 800 kWh m^{-2}, the solar potential increases, depending on the neighbourhood characteristics; the minimum from 79% (threshold value 1000 kWh m^{-2}) to 88% (threshold value 800 kWh m^{-2}) and the maximum from 94% (threshold value 1000 kWh m^{-2}) to 99% (threshold value 800 kWh m^{-2}). The results for facade-integrated PV show more sensitivity to the change of threshold values. For solar PV potential for façade the minimum increases from 3% (threshold value 800 kWh m^{-2}) to 19% (threshold value 600 kWh m^{-2}) and maximum from 20% (threshold value 800 kWh m^{-2}) to 50% (threshold value 600 kWh m^{-2}). The results for roof-integrated solar thermal collectors show that they are rather insensitive to the thresholds and do not change with lowering the threshold values. The results for facade-integrated STC, however, are very sensitive to the lowering of the threshold values. Depending on the neighbourhood characteristics, the minimum solar thermal collector potential for facades increases from 49% (threshold value 400 kWh m^{-2}) to 87% (threshold value 200 kWh m^{-2}) and maximum increases from 85% (threshold value 400 kWh m^{-2}) to 99% (threshold value 200 kWh m^{-2}). The results for passive solar potential (winter season) change as solar utilisation coefficient (η) changes from 50% ($\eta = 0.5$) to 100% ($\eta = 1$). While there is no potential for direct gain passive solar systems when the solar utilisation factor is 50% ($\eta = 0.5$), there is significant potential (from 14% to 42%) when using an utilisation factor of 100% ($\eta = 1$), which, however, is far too optimistic. In the present study, the utilisation factor of 70% ($\eta = 0.7$) is used, giving solar potential from 4% to 21%.

3.5 Model limitations

The hourly solar irradiation on each of the building surfaces calculated during one year using CitySim software is based on simplified building roof geometry. More specifically, in the simulations all the roofs are regarded as flat so as to decrease the computation time for each neighbourhood. We compared the simulation results of simplified roofs with the existing GIS model in which the details of the actual roof geometries, from the LiDAR data, were considered (www. ge.ch/sitg). Fig. 15a shows the differences between the total available roof area and the useful roof area for BiPV in each neighbourhood, using the threshold value of 1000 kWh m^{-2}. The CitySim results for the simplified flat roofs show very little difference between the total available roof area and the potential roof area for BiPV. The GIS results using LiDAR data, however, show considerable difference between the total available roof area, where the roof slope and other geometric factors are taken into account (the real roof geometry), and the useful roof area for BiPV. While the total area of the real roofs is very high, only fraction of this area has the potential of receiving above-threshold irradiation (Fig. 15a). Thus, many roof areas receive not enough solar energy and/or are poorly located for PV (e.g. because of protruding elements like chimneys).

The annual solar irradiation associated with flat roofs and sloping roofs in both models were compared. There is very little difference between total annual solar irradiation received by flat roofs and the actual roof PV potential in CitySim, considering the threshold value of 1000 kWh m^{-2}. By contrast, in the GIS model there is considerable difference between the total annual solar irradiation received by the real roofs and the actual roof PV potential, again using the threshold value of 1000 kWh m^{-2}(Fig. 15b). The lower annual solar irradiation for the real roofs, as shown in Fig. 15a, is partly because only a fraction of the total real-roof area receives enough solar energy for BiPV. However, the fraction of the real-roof area that is above the threshold value of 1000 kWh m^{-2} has comparatively high annual PV potential (Fig. 15b).

The difference between the annual solar irradiation received by the simplified roofs in CitySim and the annual solar irradiation of the real roofs modelled in GIS is 20-27%; this may be regarded as the error in using the CitySim assumption of flat roofs (Fig. 15c). However, the difference between the annual roof PV potential, using a threshold value of 1000 kWh m^{-2}, in the two models is only about 5%. Thus, simplifying roofs in CitySim so as to decrease the computation time results in a comparatively small error and may be

regarded as a valid assumption, particularly for calculating the annual solar irradiation. For a very detailed analysis, however, the comparison between the two models should be validated for monthly and hourly results. It also indicates the necessity of improving the CitySim Database Linker in order to extract roof details for the CitySim irradiation simulation. Another limitation of the model is the shadowing effects from the trees. This is particularly important for estimating the solar potentials on the building facades. This will be considered in the future development of the model.

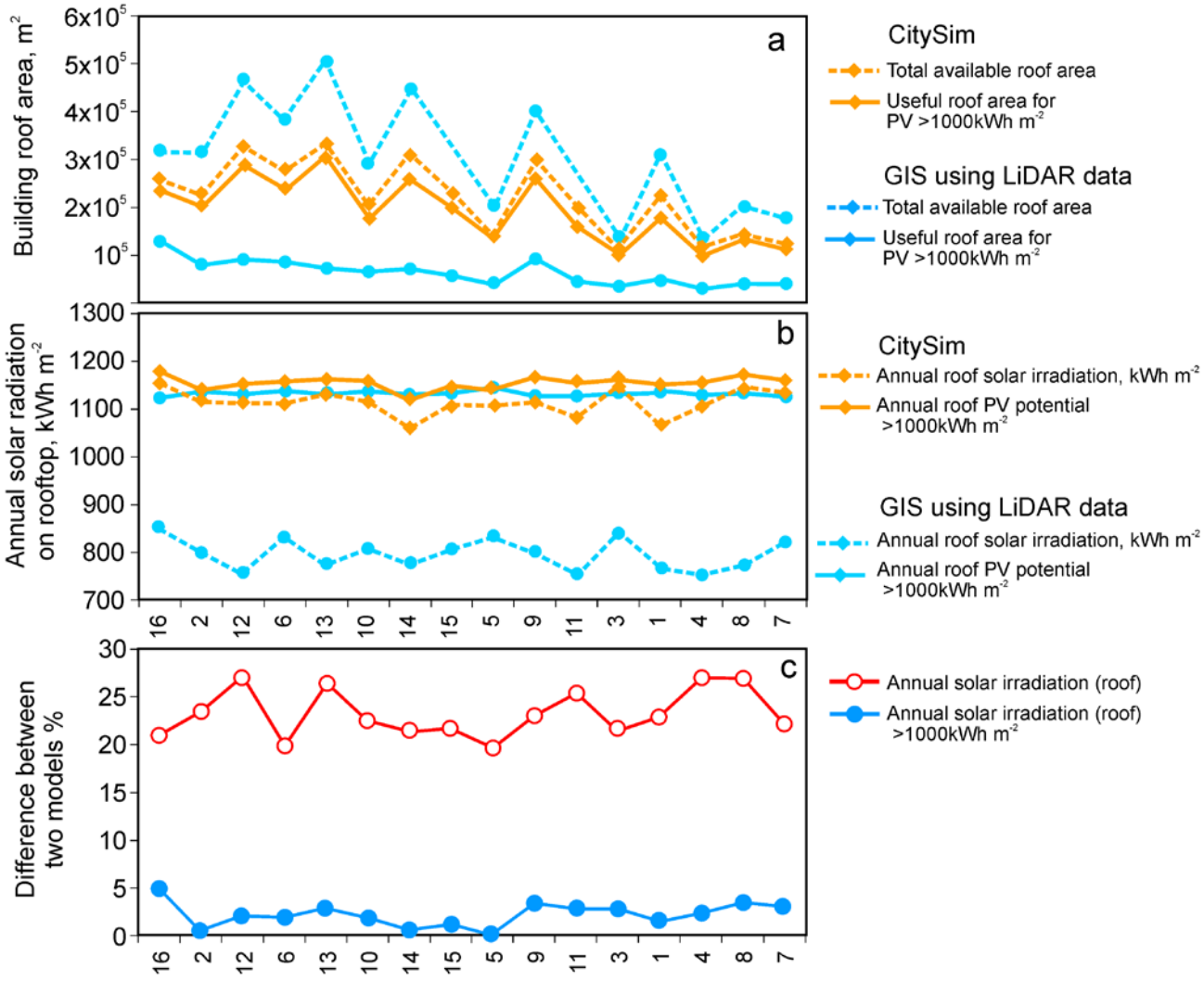

Figure 15. Comparison of computed area (a) and annual solar irradiation (b) on building roofs for photovoltaic systems simulated by CitySim (assumed flat roofs) and GIS LiDAR data (using real roofs). (c) Difference, presented as estimated percentage error, between the computed total annual solar irradiation on building roofs using CitySim (assumed flat roofs) and annual solar irradiation using GIS Lidar data (for real roofs) for photovoltaic systems.

4. Conclusion

The paper explores the implications of various compactness indicators for solar energy potential of the 16 existing neighbourhoods in city of Geneva using hourly simulations of total 11,418 buildings. The indicators are volume-area ratio, site coverage, plot ratio, building density, population density, and nearest neighbour ratio (Fig. 3). We also propose a new indicator, urban entropy, as a measure of dispersal so as to quantify the size distribution of building geometries (area, perimeter, volume, height). The impacts of all the compactness indicators on the annual solar irradiation, BiPV and STC yields as well as direct gain passive solar heating (based on hourly simulations) were then evaluated. The main findings are summarised as follows:

- The compact neighbourhoods receive a lower annual solar irradiation than dispersed neighbourhoods. The increase in annual solar irradiation, from compact to dispersed neighbourhoods, is as much as 30% to 40% depending on the compactness indicator (Figs. 5, 6). Also, the annual solar irradiation generally increases by 10-15% when moving from the compact city centre to the more dispersed suburbs.
- Increasing site coverage tends to decrease solar potential of the buildings (Fig. 5), particularly on facades, primarily due to overshadowing from neighbouring buildings (Fig. 13). PV and passive solar potentials for facade decrease as site coverage increases. The reason is partly due to overshadowing which reduces the PV and passive solar potentials on the facade in neighbourhoods with high site coverage and to a degree supressing the effects of large roof area.
- The annual solar irradiation increases with increasing the entropy of area, perimeter, and volume. Entropy is also positively related to the arithmetic average and range of the probability distributions of areas, perimeters, and volumes.
- The building orientation or azimuth varies between neighbourhoods. However, there are two main orientations, namely north east-south west and north west-south east. In the most compact neighbourhoods the annual solar irradiation is low even if the buildings are generally favourable oriented.
- The facade solar potential is much more strongly affected by the degree of compactness than the roof potential, but the actual effect depends on the solar technology considered. The main difference is due to the strong effect that mutual shading has on facades (but not on roofs). The compactness effect is very significant on facade PV and passive solar systems, but less visible for STC. Compactness has little effect on roof PV and STC.
- The annual solar irradiation for the 16 neighbourhoods increases with distance from the centre to the suburbs, primarily because of increasing solar potential on the facades (rather than the roofs). Moving from the centre, the facade PV potential increases from 3% to 20% and the facade STC potential from 49% to 85% but there is little change in STC roof potential and no change in percentage of roof potential. More specifically, the roof solar potential is similarly high in all the neighbourhoods, partly because of their due relatively uniform building-height distributions.
- Sensitivity analysis shows that decreasing the thresholds for BiPV and STC, as is likely to happen due to the future technical improvements and cost reductions, will have a large impact on the potential of facades than roofs (Figs. 11, 14). Roof solar thermal collectors are largely insensitive to threshold variation. Depending on the compactness of neighbourhoods, decreasing the threshold for facade PV, STC, and passive techniques will increase the solar potential.
- The results suggest that a production of solar energy has great potential both in compact and disperse neighbourhoods for the city of Geneva – and by implication for other cities subject to similar climate conditions. However, compact neighbourhoods in the centre of city have low potential for facades for all analysed types of solar technologies but high potential for roofs. Disperse neighbourhoods in the suburbs of the city have high solar potential for both roofs and facades as regards STC and PV.

The principal results of the present work is that, based on the example of the city of Geneva, compact neighbourhoods cast large fraction of the built environment in mutual shading, resulting in limited solar potential for retrofitting interventions on the facades. This suggests that in order to assess the solar potential for urban areas, density-related standards should be incorporated in the early stage of the design process. More specifically, an assessment is needed as to the optimal compactness of urban neighbourhoods [37, 38]. Solar-energy harvesting is considerable for roof-integrated photovoltaics and roof solar thermal collectors regardless of the compactness of neighbourhoods in Geneva, partly because of the relatively uniform building heights.

Urban areas offer great potential in many countries for harvesting solar energy, particularly using PV on the roofs of the existing buildings. The evaluation of large-scale solar potential for roofs in exiting urban areas, however, has been assessed so far for only a few countries. With rapidly expanding cities and increasing energy demand, such an assessment needs to be undertaken for many urban areas, in Switzerland and worldwide.

Acknowledgements

This research has been financially supported by CTI (Commission for Technology and Innovation) within the SCCER Future Energy Efficient Buildings and Districts, FEEB&D, (CTI.2014.0119).

References

[1] International Energy Agency. World Energy Outlook, OECD Publishing, Paris, (2014).
[2] REN21, Renewables 2015 Global Status Report, France, (2015).
[3] N. MacDowell, N. Florin, A. Buchard, J. Hallett, A. Galindo, G. Jackson, C.S. Adjiman, C.K. Williams, N. Shah, P. Fennel, An overview of CO_2 capture technologies. Energy Environ. Sci. 3 (2010) 1645–69.
[4] R. Compagnon, Solar and daylight availability in the urban fabric. Energy Build. 36 (2004) 321-328.
[5] M. Montavon, Optimisation of Urban Form by the Evaluation of the Solar Energy. PhD thesis: Ecole Polytechnique Federal De Lausanne, (2010).
[6] M. Montavon, J.L. Scartezzini, R. Compagnon, Comparison of the solar energy utilisation potential of different urban environments. In: PLEA2004-the 21st Conference on passive and low energy architecture, Eindhoven, The Netherlands, (2004) 19 -22.
[7] P. Redweik, C. Catita, M. Brito, Solar energy potential on roofs and facades in an urban landscape. Sol. Energy 97 (2013) 332–341.
[8] D. Robinson, Urban morphology and indicators of radiation availability. Sol. Energy 80 (2006) 1643-1648.
[9] V. Cheng, K. Steemers, M. Montavon, R. Energy, Urban form, density and solar potential. In: PLEA 2006-the 23rd Conference on passive and low energy architecture, Geneva, Switzerland, (2006) 1-6.
[10] V. Cheng, K. Steemers, M. Montavon, R. Compagnon, Compact cities in a sustainable manner. In: Proc. of 2nd International Solar Cities Congress, Oxford, UK, (2006) 1-11.
[11] D. Li, G. Liu, S. Liao, Solar potential in urban residential buildings, Sol. Energy 111 (2015) 225-235.
[12] J.J. Sarralde, D.J. Quinn, D. Wiesmann, K. Steemers, Solar energy and urban morphology: scenarios for increasing the renewable energy potential of neighbourhoods in London. Renew. Energy 73 (2015) 10-17.
[13] W. Pessenlehner, A. Mahdavi, Building morphology, transparence, and energy performance. In: Proc. of IBPSA-2003. 8th International Conference on Building Simulation, Eindhoven, Netherlands, (2003) 11-14.
[14] J. Kanters, M. Wall, M.C. Dubois, Typical values for active solar energy in urban planning. Energy Procedia. 48 (2014) 1607–1616.
[15] L.K. Wiginton, H.T. Nguyen, J.M. Pearce, Quantifying rooftop solar photovoltaic potential for regional renewable energy policy. Comput. Environ. Urban Syst. 34 (2010) 345–357.
[16] K.S. Lee, J.W. Lee, J.S. Lee, Feasibility study on the relation between housing density and solar accessibility and potential uses. Renew. Energy 85 (2016) 749-758.
[17] E. Nault, G. Peronato, E. Rey, M. Andersen, Review and critical analysis of early-design phase

evaluation metrics for the solar potential of neighborhood designs. Build. Environ. 92 (2015) 679-691.
[18] J.H. Kämpf, M. Montavon, J. Bunyesc, R. Bolliger, D. Robinson, Optimisation of buildings' solar irradiation availability. Sol. Energy 84 (2010) 596-603.
[19] J.H. Kämpf, D. Robinson, Optimisation of building form for solar energy utilisation using constrained evolutionary algorithms. Energy Build. 42 (2010) 807–814.
[20] Y.H. Tsai, Quantifying urban form: Compactness versus sprawl. Urban studies 42 (2005) 141-161.
[21] R. Baierlein, Atoms and Information Theory: An Introduction to Statistical Mechanics. W.H. Freeman, San Francisco, (1971).
[22] D. Kondepudi, I. Prigogine, Modern thermodynamics. Wiley, New York, (1998).
[23] P. Nelson, Biological Physics: Energy, Information, Life. W.H. Freeman, New York, (2006).
[24] E. Desurvire, Classical and Quantum Information Theory. Cambridge University Press, Cambridge, (2009).
[25] M.V. Volkenstein, Entropy and Information. Birkhauser, Berlin, (2009).
[26] N. Mohajeri, A. Gudmundsson, J.L. Scartezzini, Statistical-thermodynamics modelling of the built environment in relation to urban ecology. Ecol. Model. 307 (2015) 32–47.
[27] N. Mohajeri, A. Gudmundsson, Quantifying the differences in Geometry and size distribution of building within cities. Nexus Netw J. 16 (2014) 417-436.
[28] D. Perez, A Framework to Model and Simulate the Disaggregated Energy Flows Supplying Buildings in Urban Areas. PhD thesis: Ecole Polytechnique Federal De Lausanne, (2014).
[29] G. Upadhyay, J.H. Kämpf, J-L. Scartezzini, Ground temperature modelling: The case study of Rue des Maraîchers in Geneva, Eurographics Workshop on Urban Data Modelling and Visualisation, Strasburg, France (2014) 1-6.
[30] D. Robinson, A. Stone, Solar radiation modelling in the urban context. Sol. Energy 77 (2004) 295–309.
[31] D. Robinson, N. Campbell, W. Gaiser, K. Kabel, A. Le-Mouel, N. Morel N., J. Page, S. Stankovic, A. Stone, SUNtool - A new modelling paradigm for simulating and optimising urban sustainability. Sol. Energy. 81 (2006) 1196 -1211.
[32] D. Robinson, F. Haldi, J.H. Kämpf, P. Leroux, D. Perez, A. Rasheed, U. Wilke, CitySim: Comprehensive micro-simulation of resource flows for sustainable urban planning. In: 11th International IBPSA Conference on Building Simulation, Glasgow, Scotland, (2009) 1083 - 1090.
[33] R. Perez, R. Seals, J. Michalsky, All-weather model for sky luminance distribution—preliminary configuration and validation. Sol. Energy 50 (1993) 235–243.
[34] M.B. Pont, P. Haupt, Space Matrix: Space, Density and Urban Form. NAi Publisher, Rotterdam, Amsterdam, (2010).
[35] A. Amindarbari, A. Sevtsuk, Measuring growth and change in metropolitan form. Working paper: City Form Lab, Singapore University of Technology and Design, (2012) 2-65.
[36] D. Robinson, J.L. Scartezzini, M. Montavon, R. Compagnon, SOLURBAN project: Solar Utilisation Potential of Urban Sites. Bern: Swiss Federal Office for Energy, Bundesamt für Energie BFE, (2005).
[37] W.T. O'Brien, K.A. Kenedy, A.K. Athienitis, T.J. Kesik, The relationship between net energy and urban density of solar buildings. Environ Plann B. 37 (2010) 1002-1021.
[38] M. Batty, How tall can we go? How compact can we go? The real questions of urban sustainability. Environ Plann B. 35 (2008) 1-2.

Table 1. Summary of the descriptive statistics, urban compactness indicators, and annual solar irradiation for 16 neighbourhoods in the city of Geneva

Name	Neighbourhood ID	No. of buildings	Population density	Plot ratio	Site coverage %	Volume-area ratio	Building density	Nearest Neighbour ratio	Annual solar radiations kWh/m2	Distance from city centre, m
Bâtie – Acacias	16	420	3736	0.63	20	2.27	321	0.80	816	1690
Bouchet – Moillebeau	2	874	9401	0.67	14	2.25	546	0.86	734	2789
Champel	12	1055	10175	0.97	18	3.19	589	0.89	698	1462
Charmilles – Châtelaine	6	988	20155	1.18	24	3.86	861	1.01	708	2144
Cité – Centre	13	1193	7929	1.81	34	6.81	1195	1.00	591	793
Délices – Grottes – Montbrillant	10	638	20387	1.48	31	5.19	934	1.00	654	1466
Eaux-Vives – Lac	14	1174	15287	1.22	23	3.94	863	0.93	609	1409
Florissant – Malagnou	15	762	12406	1.06	19	3.41	654	0.97	696	1385
Grand-Pré – Vermont	5	464	16972	1.14	23	3.88	751	0.94	702	1976
Jonction	9	836	15857	1.39	30	4.95	839	0.95	659	1083
La Cluse	11	738	32596	2.19	39	6.98	1476	1.10	612	967
O.N.U.	3	181	2171	0.49	11	1.80	176	0.83	787	2862
Pâquis	1	754	21808	2.33	45	7.68	1512	1.10	598	800
Sécheron	4	272	10027	0.65	17	2.42	395	0.83	723	2289
St-Gervais – Chantepoulet	8	408	8055	1.40	25	5.24	722	0.86	626	796
St-Jean – Aire	7	661	10043	0.55	13	1.88	691	0.76	713	2231

Table 2. Summary of the descriptive statistics (average area, perimeter, volume, higher) and entropy calculations for 16 neighbourhoods in the city of Geneva

Name	Zone number	Average area, m2	Average perimeter, m	Average volume, m3	Average height, m	St. Deviation of height	Entropy of area	Entropy of perimeter	Entropy of volume	Entropy of height	Entropy of orientation
Bâtie – Acacias	16	623	87	7082	13	8	3.73	2.39	3.73	3.09	3.29
Bouchet – Moillebeau	2	260	61	4120	13	10	2.5	2.04	2.99	3.23	2.98
Champel	12	311	66	5415	15	9	2.66	2.03	3.31	3.30	3.29
Charmilles – Châtelaine	6	284	63	4480	14	9	2.53	1.93	2.78	3.19	3.27
Cité – Centre	13	286	68	5694	17	6	2.14	1.87	2.96	3.12	3.46
Délices – Grottes – Montbrillant	10	334	63	5552	16	8	3.00	2.03	3.46	3.22	3.44
Eaux-Vives – Lac	14	264	65	4566	16	8	1.94	1.58	2.52	3.21	3.29
Florissant – Malagnou	15	297	68	5215	15	10	2.31	2.00	2.85	3.28	3.19
Grand-Pré – Vermont	5	305	69	5161	16	9	2.42	1.97	2.93	3.21	3.09
Jonction	9	361	72	5898	16	8	2.89	2.06	3.21	3.13	3.29
La Cluse	11	267	64	4732	17	8	1.96	1.74	2.54	3.21	3.28
O.N.U.	3	615	94	10263	10	7	3.70	2.58	3.97	2.92	3.40
Pâquis	1	299	67	5081	16	7	2.29	1.84	2.92	3.14	2.97
Sécheron	4	418	75	6141	13	9	3.29	2.29	3.66	3.11	3.21
St-Gervais – Chantepoulet	8	351	73	7262	19	7	2.66	2.09	3.28	3.02	3.19
St-Jean – Aire	7	188	52	2725	11	8	1.95	1.74	2.37	3.02	3.20

Table 3. Relative fraction of building facade and roof areas appropriate for a given solar technology in the 16 neighborhood of the city of Geneva

Geneva city		Photovoltaic systems %		Solar thermal collector%		Passive solar heating techniques %
Neighbourhood	ID	Façade (annual)	Roof (annual)	Façade (annual)	Roof (annual)	Façade (winter)
Bâtie – Acacias	16	15	93	79	99	15
Bouchet – Moillebeau	2	20	91	85	100	21
Champel	12	12	89	74	98	12
Charmilles – Châtelaine	6	10	86	74	99	12
Cité – Centre	13	6	93	49	97	6
Délices – Grottes – Montbrillant	10	6	88	61	98	8
Eaux-Vives – Lac	14	7	84	55	95	8
Florissant – Malagnou	15	12	88	77	99	14
Grand-Pré – Vermont	5	16	87	76	99	15
Jonction	9	7	87	59	98	8
La Cluse	11	6	82	57	97	4
O.N.U.	3	15	94	80	99	15
Pâquis	1	3	79	50	95	4
Sécheron	4	9	87	70	98	10
St-Gervais – Chantepoulet	8	10	94	53	98	11
St-Jean – Aire	7	14	91	76	99	16

Table 4. Annual solar irradiation ($kWhm^{-2}$) threshold values used when computing the potential for the corresponding solar techniques. The threshold values indicated in bold are used in Figures 12 and 13.

Solar technology		Threshold for systems on facades	Threshold for systems on roofs
Passive	Passive solar heating (winter)	131 kWh m^{-2}, η = 1.0 (UF)	-
		187 kWh m^{-2} η = 0.7 (UF)	-
		262 kWh m^{-2} η = 0.5 (UF)	-
Active	Photovoltaic systems (annual)	**800 kWh m^{-2}**	**1000 kWh m^{-2}**
		700 kWh m^{-2}	900 kWh m^{-2}
		600 kWh m^{-2}	800 kWh m^{-2}
	Solar thermal collectors (annual)	**400 kWh m^{-2}**	**600 kWh m^{-2}**
		300 kWh m^{-2}	500 kWh m^{-2}
		200 kWh m^{-2}	400 kWh m^{-2}